Electrospark deposition interlayers for dissimilar resistance welding of steel to aluminum

Pablo D. Enrique *[a], Caiyin Li [a], Christopher DiGiovanni [a], Stephen Peterkin [b], Norman Y. Zhou [a]

* Corresponding Author: pdenriqu@uwaterloo.ca

[a] University of Waterloo, 200 University Ave W, Waterloo, Ontario, N2L 3G1, Canada.

[b] Huys Industries Ltd., 175 Toryork Drive, Unit 35 Weston, Ontario, M9L 1X9, Canada.

This is an author generated post-print of the article:

P.D. Enrique, C. Li, C. DiGiovanni, S. Peterkin, N.Y. Zhou, Electrospark deposition interlayers for dissimilar resistance welding of steel to aluminum, Manuf. Lett. 24 (2020) 123–126. doi:10.1016/j.mfglet.2020.04.009.

Abstract

The transportation industry is facing increasing pressure to lightweight vehicles and improve fuel economy. One option is the use of low-density aluminum alloys rather than steels. However, adoption of aluminum alloys is hampered by challenges during the welding of aluminum to steel. Here, an electrospark deposition AA4043 interlayer is applied for the dissimilar resistance spot welding of an aluminum alloy (AA5052) to a galvanized dual phase steel (GI DP600). A minimum 30% tensile lap-shear strength increase is obtained using this interlayer. This manufacturing technique has the potential to allow for greater adoption of aluminum alloys in vehicle lightweighting applications.

Keywords: Resistance spot welding, dissimilar welding, interlayer, electrospark deposition, aluminum/steel

---

Introduction

With a density almost 3 times less than typical advanced high strength steels, aluminum alloys provide vehicle manufacturers with an attractive option for reducing vehicle weight. However, difficulties joining these dissimilar metals have impeded the replacement of steel parts with lighter aluminum alloy counterparts. Literature studies have identified several challenges associated with welding the two materials. The lower relative melting temperature of aluminum alloys results in bonding along a liquid aluminum and solid iron interface, similar to a brazing process [1]. This solid/liquid interface encourages the dissolution of iron and the formation of brittle intermetallics, with the aluminum-rich intermetallics Al_5Fe_2 and $Al_{13}Fe_4$ being more detrimental than their iron-rich counterparts [1,2]. Controlling the thickness and type of intermetallic layer that forms between the two metals is critical to improving the strength and quality of aluminum alloy to steel welds.

Several studies have been reported in literature that attempt to resolve the formation of brittle intermetallics. The use of galvanized steel was found to form a thinner intermetallic than uncoated steel when welded to an aluminum alloy, attributed to energy absorption by the evaporation of the zinc coating. This thinner intermetallic, along with fragmentation of the intermetallic layer, resulted in a notable strength increase [3]. The use of an aluminum interlayer applied to a steel sheet prior to resistance welding is also effective at increasing weld strength, since the resistance weld occurs between the aluminum alloy sheet and the interlayer rather than the steel sheet. Application of the interlayer to the steel sheet must be performed with a low heat input technique such as ultrasonic welding [4] or cold spraying [5]. With reduced heat input or faster cooling, aluminum spends less time in the molten state and intermetallic growth is hindered [6].

In this work, an electrospark deposition (ESD) process is used to apply an AA4043 interlayer onto a galvanized (GI) DP600 sheet prior to resistance welding with an AA5052 sheet. ESD operates by discharging a capacitor through a welding rod and workpiece sheet, creating a short-duration arc that transfers droplets of material from the welding rod onto the workpiece [7]. With repeated capacitor discharge, the small droplets are layered to form thicker coatings. Due to the small droplet size and short pulse durations, cooling rates are high and heat buildup is limited [8]. ESD AA4043 interlayers are shown in this study to result in stronger resistance spot welds than their interlayer-free counterparts.

Materials and Methods

Commercially available welding rods of AA4043 with 1.8 mm diameter are deposited onto 1.2 mm sheets of GI DP600 using a Huys Industries ESD machine. The ESD process parameters of 310 µF and 140 V are chosen to obtain the fastest deposition rate with a 150 Hz frequency. These parameters were obtained by depositing coatings in 1 cm^2 areas on a GI DP600 sheet, measuring the thickness of the coating after cross sectioning, and using the deposition time for each set of parameters to calculate the deposition rate. An average of 40 measurements per sample was used to find the coating thickness, with images taken on an Oxford BX51M optical microscope and measurements made using ImageJ software. During all depositions, ultra high purity argon gas was applied coaxially with the welding rod at a flow rate of 10 L/min.

Resistance spot welding of AA5052 to GI DP600 or AA4043 coated GI DP600 was performed as shown in Figure 1a,b. Copper class II electrodes provided by Huys Industries with a contact diameter of 6 mm were used on a 60 Hz alternating current (AC) resistance spot welder, with a welding current from 9-15 kA, an electrode force of 3 kN, pre-squeeze time of 50 cycles (one cycle = 16.67 ms), weld time of 20 cycles, post-weld hold time of 20 cycles, and water cooling flow rate of 5 L/min. For samples with the AA4043 interlayer, an ESD processing time of 70 s was used to coat a circle with 1.5 cm diameter for a target coating thickness of 0.7 mm.

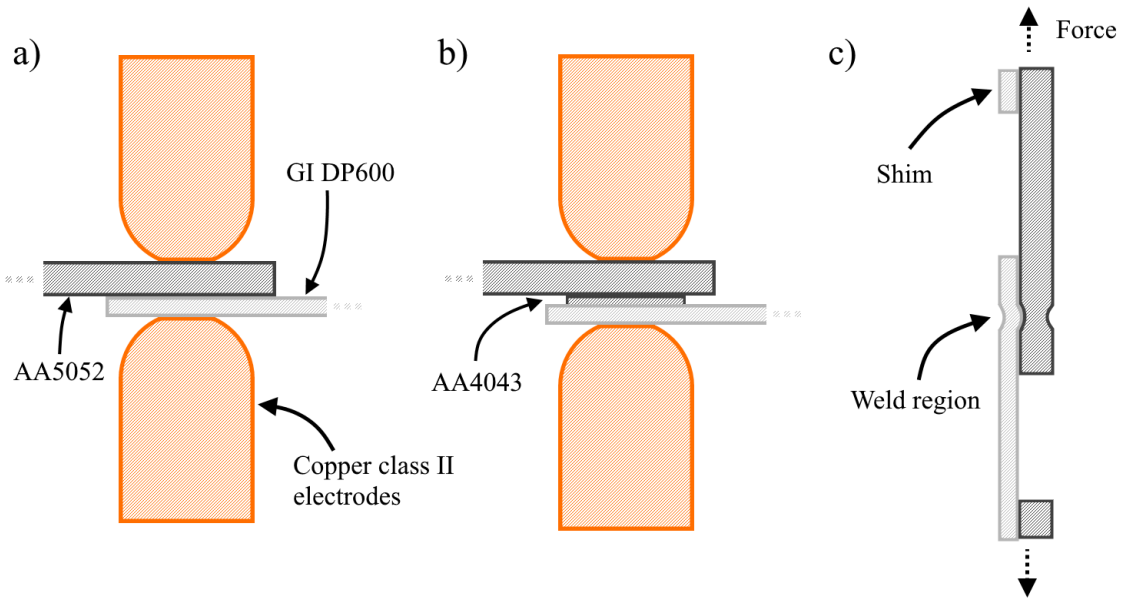

Figure 1. Schematic of resistance spot welding (RSW) process for a) AA5052 to GI DP600, b) AA5052 to GI DP600 with an AA4043 interlayer and c) the tensile lap-shear testing condition

Weld strengths are measured using tensile lap-shear coupons in a Tinius Olsen H10KT tensile tester. A weld was performed at the center of a 4 cm overlap between a sheet of AA5052 and GI DP600 as shown in Figure 1c. Shims were used during tensile testing to prevent eccentricity during loading. Characterization of cross sections are performed using a Zeiss UltraPlus scanning electron microscope (SEM) with an AMETEK energy-dispersive X-ray spectroscopy (EDX) attachment.

Results and Discussion

To determine the appropriate ESD parameters for deposition of an interlayer, a parameter optimization study was first performed, the results of which are presented in Figure 2. An increase in capacitance (C) and voltage (V) increases energy input (E) according to the equation for energy stored in a capacitor ($E = \frac{1}{2}CV^2$), which transfers greater amounts of material to the substrate. Parameters which result in the highest deposition rate were chosen to reduce the time required for interlayer application.

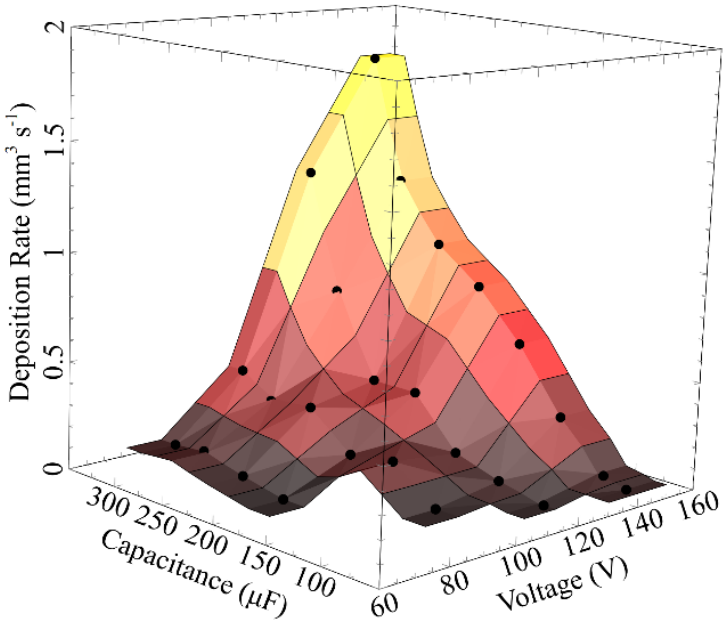

Figure 2. Deposition rate for AA4043 on GI DP600 with a fixed frequency (150 Hz)

The application of an ESD interlayer between DP600 and AA5052 prior to RSW was found to benefit the weld strength in two ways. Due to localized heating during the ESD process, the zinc coating typically present on GI DP600 is removed. With no visual evidence of a zinc layer after ESD and no detection of zinc via EDX in the aluminum ESD interlayer, vaporization is likely responsible for the removal of the zinc. However, a small amount of zinc below the EDX detection limit may have solutionized in the deposited aluminum interlayer. In welds produced without an interlayer, zinc remains on the DP600 sheet during resistance welding. As heat is generated at the faying interface the following physical changes occur:

$$Zinc\ melting\ (419\ °C) \rightarrow AA5052\ melting\ (607\ °C) \rightarrow Zinc\ boiling\ (907\ °C) \quad [1]$$

Heat generated during welding is first used to melt the zinc coating, which decreases the contact resistance and reduces the amount of additional heat generated. This limits the amount of heat available to melt the AA5052, which limits the size of the weld nugget. To overcome this issue, higher welding currents must be used. However, too much heat generation results in boiling of the zinc coating. This leads to the formation of gas porosities that remain trapped within the AA5052 sheet after welding [3]. Removal of zinc during ESD prevents the zinc-related phase changes from influencing the weld. The second benefit is a change in the weld interface; rather than welding of an aluminum alloy to steel, the resistance welding process instead joins an aluminum alloy to another aluminum alloy when an interlayer is used. This avoids a large heat generation at the aluminum/steel interface that would result in iron aluminide intermetallic growth.

The benefits of using an AA4043 interlayer is evident in the tensile lap-shear testing results. Welds of AA5052 to GI DP600 are stronger when welded with an AA4043 interlayer across all trialed currents (Figure 3), with a minimum average increase of 30%. The lowest current of 9 kA is insufficient to form a weld in the samples without an interlayer, attributed to insufficient heat generation for both melting of the zinc coating and melting of the aluminum. This finding confirms previous studies in which welding was attempted but not successful at 9 kA on zinc coated steel [3]. With the application of an AA4043 interlayer, 9 kA is sufficient for some joining to occur and an average failure load above 5 kN is obtained with a weld current as low as 11 kA. Without the use of an interlayer, the failure load remains consistently lower, reaching an average of 4.3 kN at a weld current of 15 kA. Interfacial failure occurs in all samples regardless of the weld current or whether an interlayer was used. The difference in strength is attributed to differences in the thickness of the intermetallic that forms during welding.

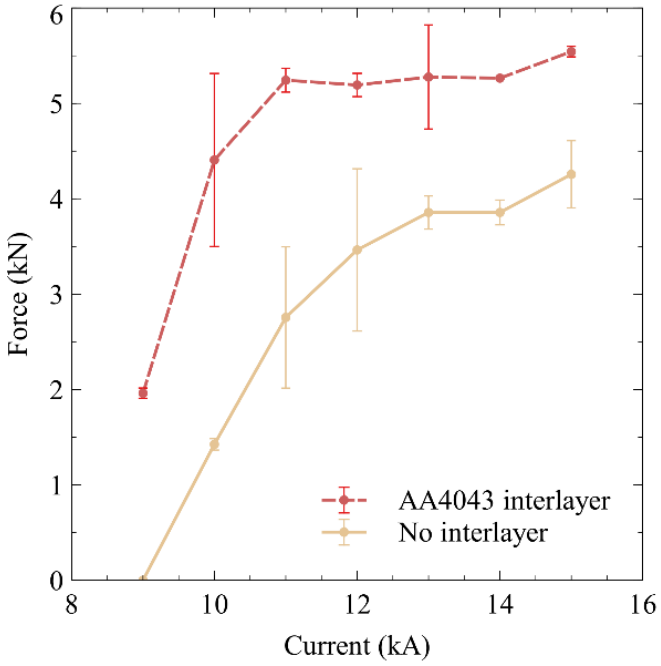

Figure 3. tensile lap-shear test for AA5052 to GI DP600 with and without an AA4043 interlayer

The aluminum alloy to steel interface has a noticeably thinner iron aluminide intermetallic when resistance spot welded with the AA4043 interlayer. At the highest welding current of 15 kA, a sub-micrometer thick intermetallic (Figure 4a) is present that matches the intermetallic thickness formed during the deposition of the interlayer (Figure 4b). This suggests that growth of this intermetallic during resistance spot welding is limited. A comparison to the intermetallic that forms after welding without an interlayer is shown in Figure 4c, which ranges from 1 to 9 µm thick. Due to the larger thickness, a more reliable EDX measure of this intermetallic can be obtained, which indicates an average composition of approximately 63 wt% Al and 37 wt% Fe.

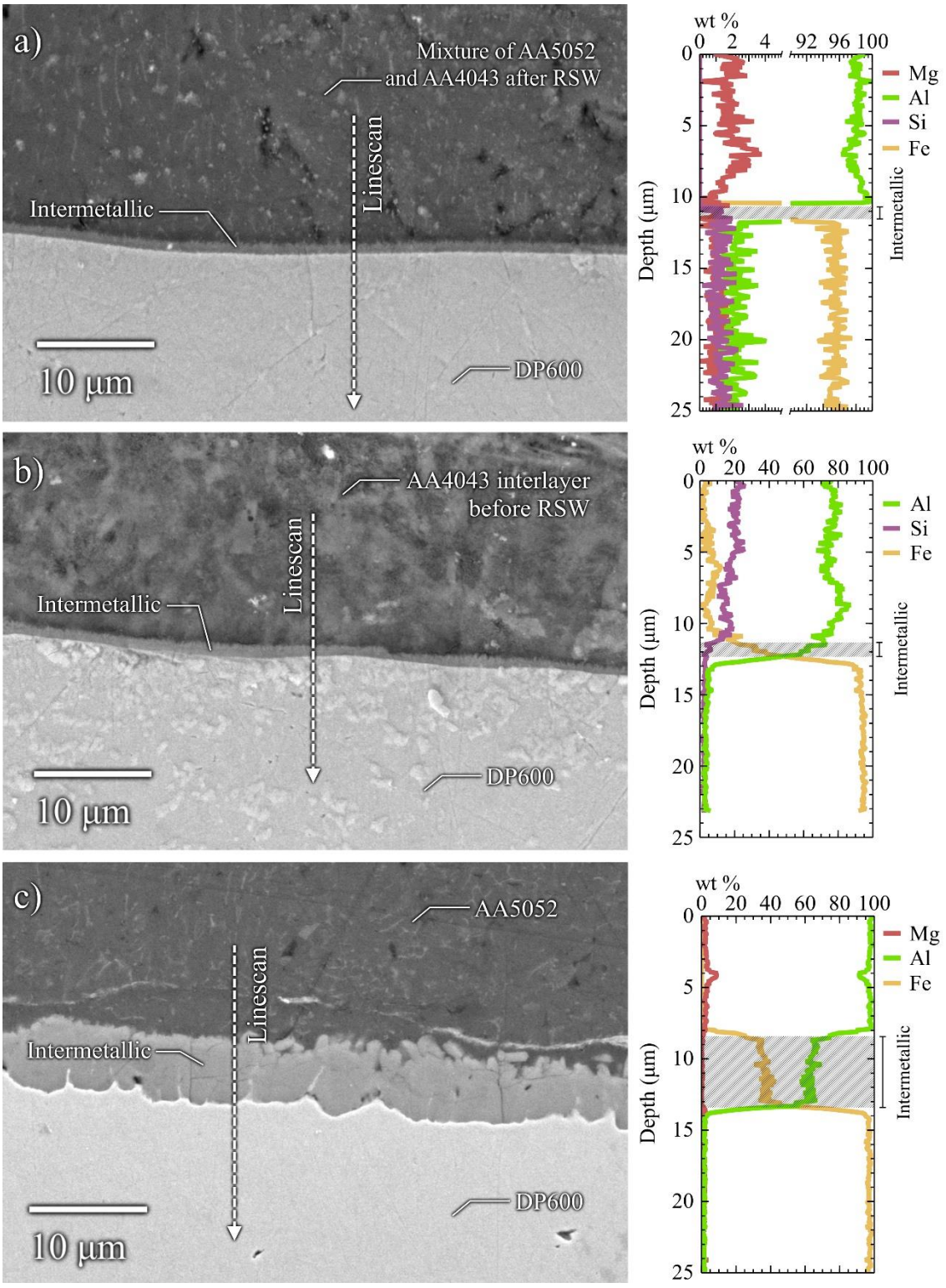

Figure 4. SEM images of a) AA5052 welded to AA4043 coated GI DP600 at 15 kA b) ESD of AA4043 on GI DP600 before RSW and c) AA5052 welded to GI DP600 without an interlayer at 15 kA. Results of the EDX linescan as indicated in each image are shown adjacent to the image.

Based on the EDX linescans indicated by the dashed arrows in Figure 4a, b, the AA4043 interlayer fully melts during the resistance welding process. Although AA4043 contains silicon – which can be detected in the interlayer prior to RSW (Figure 4b) – none is detected in the aluminum adjacent to the intermetallic after RSW (Figure 4a). Instead, EDX reveals magnesium (Figure 4a) which can be attributed to AA5052. Therefore, the following is proposed to explain the difference in iron aluminide intermetallic thickness between sheets with and without an interlayer: heat generated during welding due to the contact resistance between AA5052 and AA4043 is firstly used to melt the contact asperities between the two interfaces and then used to melt the AA4043 interlayer. These two energy sinks act as a barrier to the energy required for iron aluminide intermetallic growth at the aluminum alloy to steel interface. Instead, the intermetallic identified at that interface is unchanged from that formed during ESD interlayer application, as can be seen by comparing Figure 4a and Figure 4b.

Conclusions

The use of electrospark deposition (ESD) for the application of interlayers is demonstrated for the resistance spot welding of an AA5052 sheet to a galvanized DP600 sheet. A comparison of weld strength with and without an AA4043 interlayer shows a minimum 30% improvement in tensile lap-shear strength when the interlayer is used, attributed to the presence of a thinner iron aluminum intermetallic at the faying surfaces. Additionally, with the application of an interlayer, an initial weld and a full weld strength were both achieved at lower welding currents than without the interlayer.

Acknowledgements

This work was performed with funding support from the Natural Sciences and Engineering Research Council of Canada (NSERC), Huys Industries and the CWB Welding Foundation, in the Centre for Advanced Materials Joining at the University of Waterloo.

References

[1] Pouranvari M. Critical assessment: dissimilar resistance spot welding of aluminium/steel: challenges and opportunities. Mater Sci Technol (United Kingdom) 2017;33:1705–12. doi:10.1080/02670836.2017.1334310.

[2] Zhang WH, Qiu XM, Sun DQ, Han LJ. Effects of resistance spot welding parameters on microstructures and mechanical properties of dissimilar material joints of galvanised high strength steel and aluminium alloy. Sci Technol Weld Join 2011;16:153–61. doi:10.1179/1362171810Y.0000000009.

[3] Arghavani MR, Movahedi M, Kokabi AH. Role of zinc layer in resistance spot welding of aluminium to steel. Mater Des 2016;102:106–14. doi:10.1016/j.matdes.2016.04.033.

[4] Lu Y, Mayton E, Song H, Kimchi M, Zhang W. Dissimilar metal joining of aluminum to steel by ultrasonic plus resistance spot welding - Microstructure and mechanical properties. Mater Des 2019;165:107585. doi:10.1016/j.matdes.2019.107585.

[5] Winnicki M, Małachowska A, Korzeniowski M, Jasiorski M, Baszczuk A. Aluminium to steel resistance spot welding with cold sprayed interlayer. Surf Eng 2018;34:235–42. doi:10.1080/02670844.2016.1271579.

[6] Borrisutthekul R, Yachi T, Miyashita Y, Mutoh Y. Suppression of intermetallic reaction layer formation by controlling heat flow in dissimilar joining of steel and aluminum alloy. Mater Sci Eng A 2007;467:108–13. doi:10.1016/j.msea.2007.03.049.

[7] Tang SK. The Process Fundamentals and Parameters of Electro-Spark Deposition. University of Waterloo, 2009.

[8] Gould J. Application of Electro-Spark Deposition as a Joining Technology. Weld J 2011;90:191–7.